Manufacturing Rev. **9**, 31 (2022)

https://doi.org/10.1051/mfreview/2022029

Manufacturing Review
Available online at:
https://mfr.edp-open.org

RESEARCH ARTICLE OPEN ACCESS

Evaluation of mechanical behaviour and tensile failure analysis of 8 wt.% of nano B_4C particles reinforced Al2214 alloy nano composites

Kumar Gopalan[1], Saravanan Rajabathar[1], Madeva Nagaral[2,*], and Hemnath Raju Thippeswamy[3]

[1] Mechanical Engineering Department, University Visvesvaraya College of Engineering, Bangalore University, Bangalore, 560001, Karnataka, India
[2] Aircraft Research and Design Centre, Hindustan Aeronautics Limited, Bangalore 560037, Karnataka, India
[3] Department of Mechanical Engineering, New Horizon College of Engineering, Bangalore 560103, Karnataka, India

Received: 13 April 2022 / Accepted: 2 September 2022

Abstract. The microstructure and mechanical properties of Al2214-8 wt.% of 500 nm sized B_4C particles reinforced composites were studied in this study. By using a liquid metallurgical process, composites containing 8 wt.% of B_4C in Al2214 alloy were created. To increase the wettability and dispersion of the composites, fortification particles were warmed to 300 °C and then added in groups of two into the vortex of liquid Al2214 alloy compound. ASTM standards were used to analyse the mechanical characteristics of Al2214 alloy and Al2214-8 wt.% of B_4C composites. The distribution and presence of nano B_4C particles in the Al2214 alloy matrix were confirmed by microstructural analysis using SEM and EDS. XRD patterns indicated the presence of the B_4C phases in Al2214 alloy composites. The addition of 8 wt.% of B_4C particles to Al2214 alloy improved its hardness, ultimate, yield, and compression strength. Furthermore, the presence of B_4C particles reduced the ductility of the Al2214 alloy. The tested materials were subjected to tensile fractography to determine the various fracture mechanisms.

Keywords: Al2214 alloy / B_4C nano particles / microstructure / tensile strength / fractography

1 Introduction

Bearings, piston rings, brake pads, clutches, couplings, and gears, among other things, must have a long service life, be reliable, and have minimal friction. These parts operating conditions vary depending on a variety of factors such as sliding speeds, weights, ambient conditions, and other factors. There is no single metal that can meet all of the requirements. As a result, it's critical to create a composite material with all of the necessary combinational properties to meet engineering criteria. Aluminium composites have gained worldwide attention in the field of research in military applications such as armour tanks, bullet proof jackets, automobile body parts, aeronautical applications, space, and the automotive industries due to their enriched possessions such as high strength, lightweight, and excellent wear resistance [1–3]. Due to their superior strength-to-weight ratio, heat treatable aluminium alloys such as Al2214, Al6063, and Al7075 are often used, and metal matrix composites (MMCs) manufactured with these alloys have improved temperature stability [4,5]. Aluminum metal matrix composites (AMMC) properties can be enhanced by selecting the appropriate reinforcing geometry, type, and shape, as well as the appropriate fabrication procedure [6,7]. The addition of hard and stronger ceramic particles to a medium-strength, ductile, and low-stiffness metal matrix can improve the properties of the ceramic and the base matrix [8,9]. The qualities of MMCs are largely determined by the processing method used. The processing approaches for manufacturing composites are determined by whether the reinforcement is added to the matrix in a solid or liquid state [10,11]. Stir casting is a favoured processing technique for fabricating composites in the liquid state because of its flexibility, economy, and ability to create bulk quality production [12,13]. The liquid state technique works on the premise of melting the matrix material, then adding reinforcement to the melt to get the desired dispersion [14].

There are a number of problems to consider when fabricating MMCs by stir casting, including wettability, porosity during solidification, and cluster due to non-uniformity [15]. To achieve homogeneity, homogeneous reinforcement mixing must be concentrated. While

* e-mail: madev.nagaral@gmail.com

Table 1. Chemistry of Al2214 Alloy.

Elements	Si	Fe	Cu	Mg	Cr	Zn	Ti	Mn	Al
Weight (%)	1.0	0.3	5.0	0.8	0.10	0	0.10	0.4	Bal

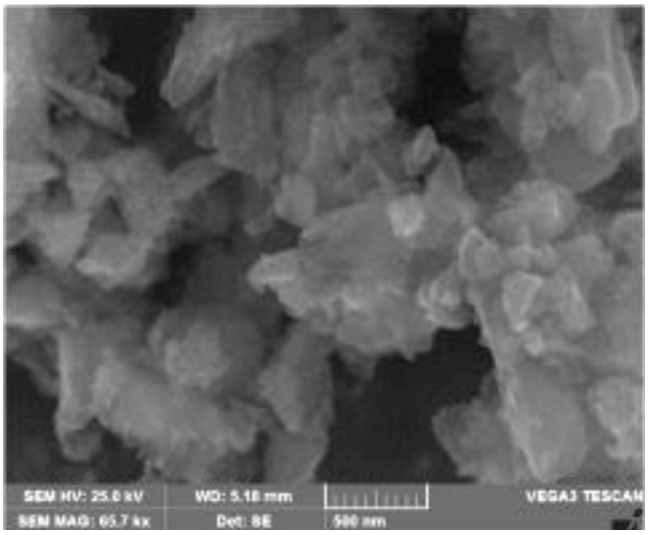

Fig. 1. SEM micrograph of B_4C particles.

fabricating, high wettability between two phases and good bonding must be optimised. Among the numerous matrix materials, Al and its alloys are widely used in the production of MMCs for industrial applications. Different combinations of Al based MMCs with different particles B_4C, Al_2O_3, SiC, WC, and TiB_2 are used to generate MMCs with required qualities [16–18]. Boron carbide is a hard ceramic particle that is utilised for high-temperature applications and is one of the most important hard ceramic particulate reinforcements for Al alloy matrixes [19]. Boron carbide is a refractory metal with a specific density of 2.52 g/cc that is used in cutting tools, extrusion dies, and high-temperature drilling [20].

Using 500 nm sized B_4C particles in an Al2214 alloy matrix, a limited investigation was carried out based on the available literature. Stir casting is used to make the Al2214 with 8 wt.% of B_4C metal matrix composite. To avoid agglomeration, B_4C particles are added to the aluminium melt in two phases. The prepared composites are next put through a series of mechanical testing.

2 Experimental details

2.1 Materials used

Al2214 alloy is a wrought alloy that can be processed in a secondary manner. Copper is the principal alloying element in Al2214, with a melting point of 660 °C and a density of 2.80 g/cm^3. The Al2214 alloy is mostly employed in the transportation and aerospace industries, among other things. Al2214 is robust, corrosion-resistant, and has high raised temperature strength, as well as a high self-healing capability during the welding process. Al2214's chemical composition is shown in Table 1.

The reinforcement material is 500 nm boron carbide obtained from Speedfam Chennai Ltd. in India. The density of the reinforcement particle is 2.52 g/cm^3, with a melting point of 3300 °C and a hardness of 3100–3600 kg/mm^2. The SEM and EDS spectrum of B_4C particles utilised to make the composites are shown in Figures 1 and 2.

2.2 Methodology and testing

The Al2214-B_4C composites are made using the stir casting process. In a graphite crucible, a measured amount of Al2214 alloy is put. After that, the crucible is placed in the electric furnace. To melt the Al2214 alloy, the furnace is kept at 750 °C. B_4C particles are roasted at 300 °C in a separate oven at the same time to reduce moisture content and promote wettability. Hexochlorthane [21], a degassing agent, is applied to the molten metal to prevent undesired gases [22]. A unique two-step reinforcement addition approach is used to pour a known quantity of B_4C particles into molten metal. The casting is then swirled for 5 min at 300 rpm with a mechanical stirrer made of zirconium coated material for a homogeneous mixture. The molten metal is put into the mould die right away. Cast iron is used to make the die. The cast iron die has a length of 120 mm and a diameter of 15 mm. To carry out the relevant testing, the castings are machined to ASTM standards. Figure 3 shows the composites that were prepared for the investigation.

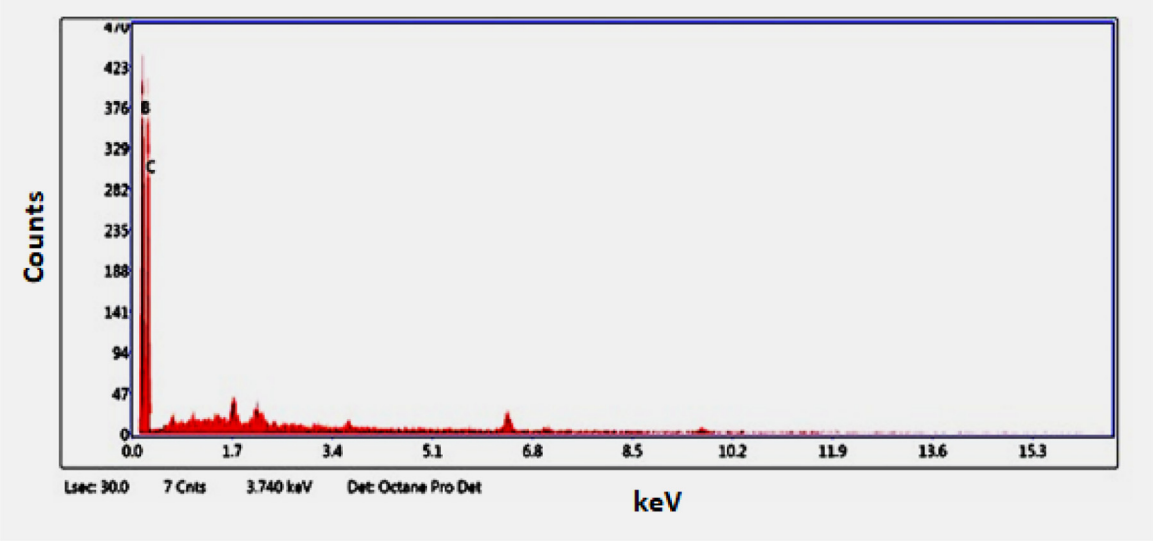

Fig. 2. EDS spectrum of B_4C particles.

Fig. 3. Al2214-B_4C composite after casting.

Following casting, the sample is processed for microstructural analysis using an electron microscope to determine the uniform distribution of B_4C particles in the Al2214 alloy. Microstructure pictures of Al2214 alloy and Al2214-B_4C composites are acquired. Microstructure specimen dimensions are 12 mm in dia., and 5 mm in height. 300, 600, and 1000 grit paper are used to grind the specimen's surface. The surface is then polished on a polishing machine with a polishing paper for a smoother finish. Following that, the specimens are washed with distilled water to eliminate any foreign particles such as dirt or other impurities that may have accumulated on the polished surface. Keller's reagent [23] is used to etch the specimens to create a contrast surface. XRD studies are carried out by a PANALYTICAL XRD using Cu-K alpha radiation. The 2θ range is selected such that all the intense peaks of the material phases predictable are covered.

The specimen is machined in accordance with ASTM standard E10 [24] for the hardness test. The Brinell hardness tester is used to test the hardness. The polished surface of the specimen is smooth. A 5 mm ball depression was made on the specimen, and a 250 kg force was applied. On the surface of the specimen, five indentation marks are made, and the findings are analysed.

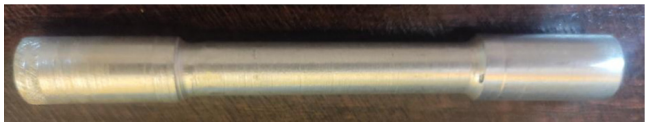

Fig. 4. Sample of the tensile test specimen.

The specimens are machined according to ASTM standard E8 [25] to assess the tensile behavior of as cast Al2214 alloy its B_4C composites. To achieve precise findings, three samples are tested for tensile strength testing. The computer-integrated machine is used to test tensile strength, explore the behavior of Al2214-B_4C composites under unidirectional tension, and study the influence of uniform distribution. The specimen measures overall length of 104, with gauge length of 45 mm, and 9 mm in gauge diameter. This tensile test can be used to study the mechanical behavior of cast alloys and composites in order to determine ultimate, yield, and elongation. Compression test is conducted as per ASTM E9 standard on specimen with dimensions of 15 mm diameter and 22.5 mm in length. Figure 4 shows the tensile test specimen.

3 Results and discussion

3.1 Microstructural Studies

Scanning electron microphotographs of Al2214 alloy and composites with 8 wt.% of B_4C particles are shown in Figures 5a and 5b. The SEM picture of Al2214 alloy is shown in Figure 5a. This denotes the absence of particles and the presence of clean grain boundaries. There are no voids or other casting flaws visible on the microscope. Microphotographs of Al2214-8 wt.% of B_4C composite are shown in Figure 5b. The B_4C particles, which are observable in the micrographs, are found in 8 wt.% of B_4C reinforced composites, according to the micrograph.

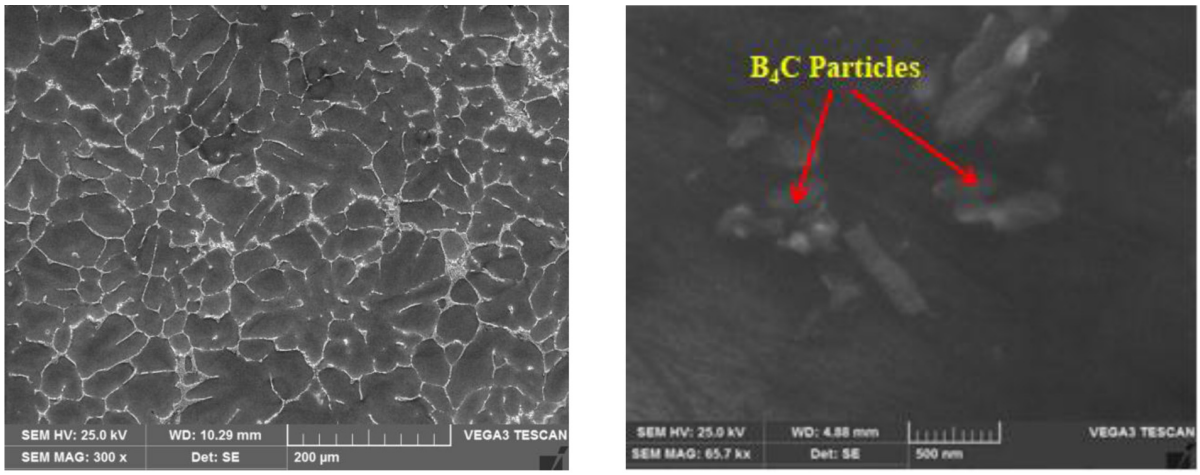

Fig. 5. Scanning electron microphotographs of (a) as cast Al2214 alloy (b) Al2214-8 wt.% of B_4C composites.

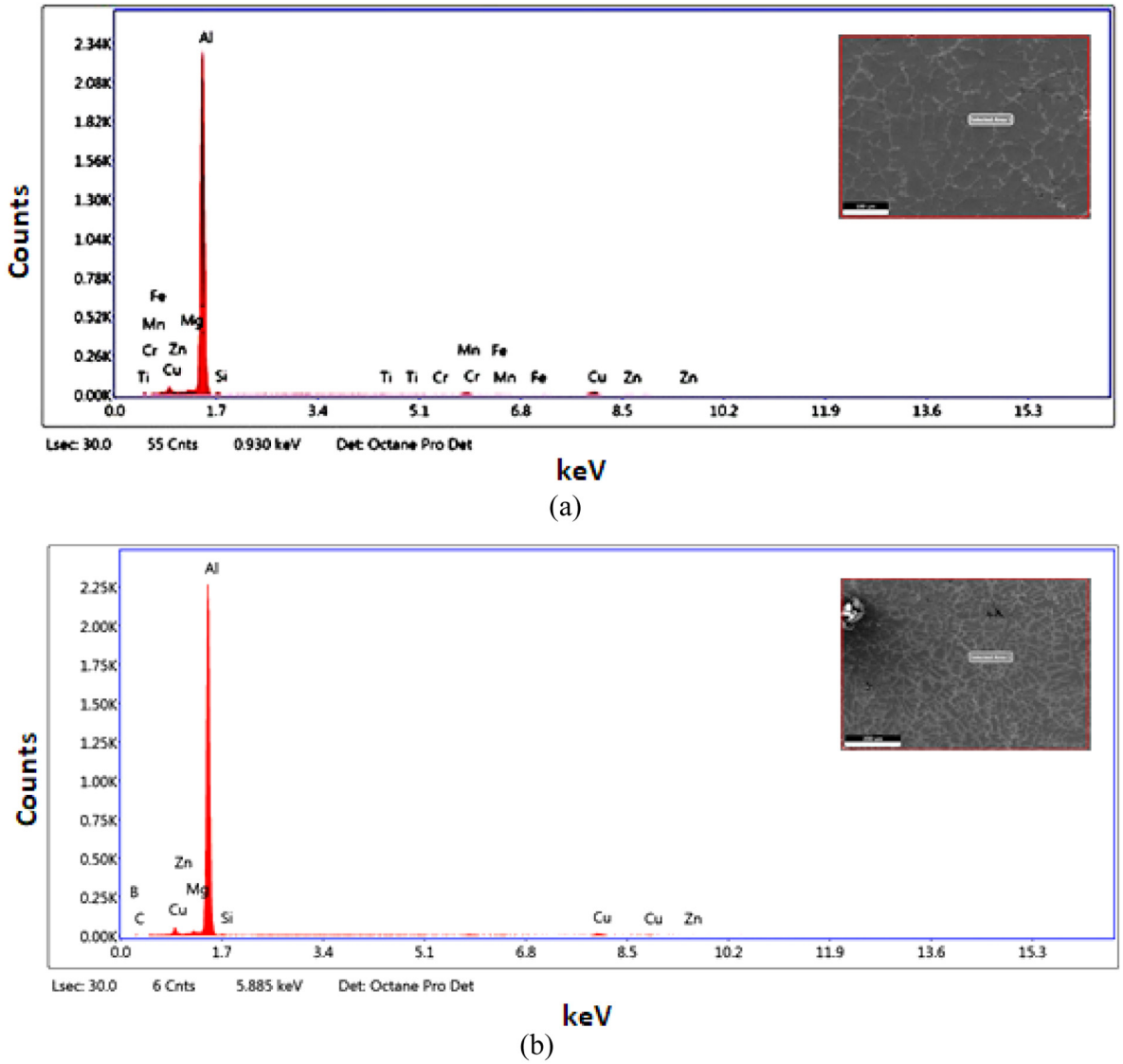

Fig. 6. EDS spectrum of (a) Al7049 alloy (b) Al7049-8 wt.% of B_4C composites.

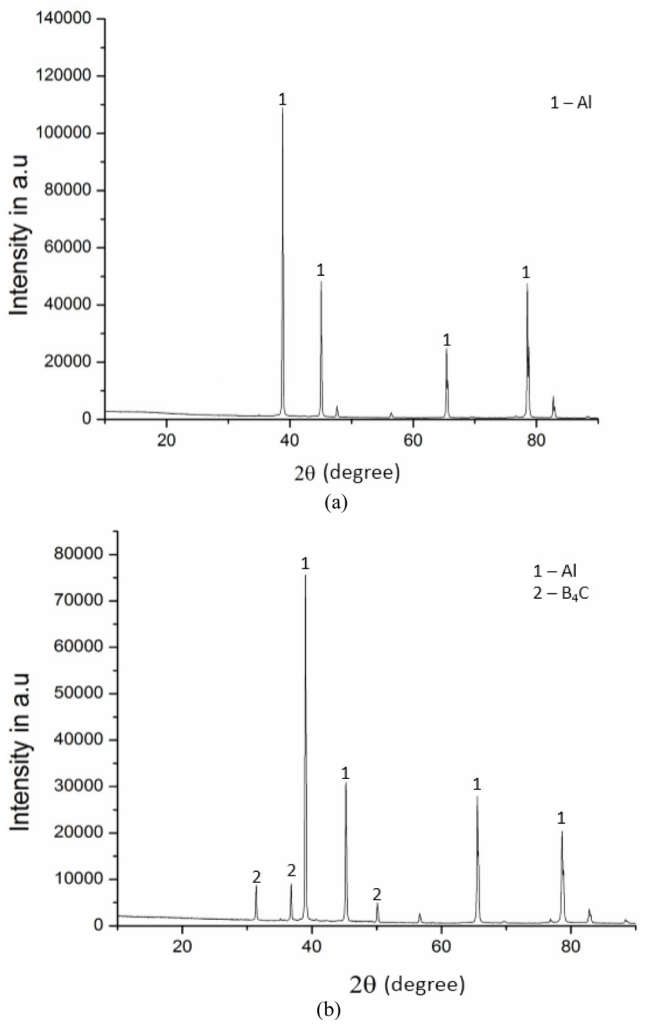

Fig. 7. X-ray diffraction patterns of (a) Al2214 alloy (b) Al2214-8 wt.% of B_4C composites.

Because of the revolutionary two-stage technique used to create the composites; these particles are devoid of clustering. The presence of these nano B_4C particles increases the Al2214 alloy's mechanical properties [26].

The EDS spectrum of Al2214 alloy and 8 wt. percent nano B_4C composites is shown in Figures 6a and 6b. Cu, along with Si, F, and Mg, is a key alloying ingredient in Al2214 alloy, as seen in Figure 6a. The EDS spectrum of Al2214-8 wt.% of B_4C nano composites is also shown in Figure 6b. The occurrence of B_4C particles in the Al2214 alloy in the form of B and C elements was detected in the EDS spectra of composites. The inclusion of B and C elements, as well as Zn, Mg, Fe, and Si, verifies the validity of the casting approach used to create the composites.

The Al2214 alloy and Al2214-8 wt.% of B_4C composites are analysed using an X-Ray Diffractometer. The XRD pattern of Al2214 is given in Figure 7a; typically, aluminium phases are existing at various peaks, as seen in Figure 7a. At 39, 45, 65, and 79, the presence of Al phases is confirmed with varying intensities. At 39, the Al phase has the highest intensity. The XRD pattern of Al2214-8 wt.% of B_4C composites is shown in Figure 7b.

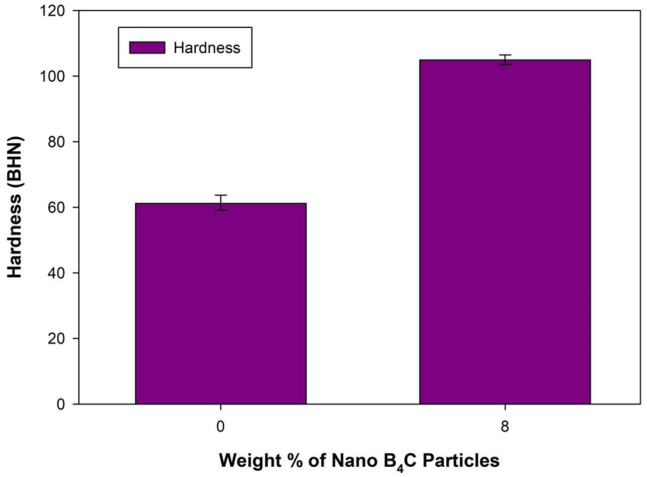

Fig. 8. Hardness of Al2214alloy and B_4C reinforced composites.

The various phases, such as Al and B_4C, are shown in Figure 7b. As previously said, Al phases are widely available at various 2 angles with varying intensities, whereas B_4C particle phases are identified at 31 degrees, 38 degrees, and 50 degrees with varying intensities.

3.2 Hardness measurements

Figure 8 and Table 2 display the hardness of Al2214 alloy and Al2214 with 8% B_4C composites. The plot shows that adding 8 wt.% of B_4C particles to the Al2214 alloy improves its hardness. The hardness of the alloy as cast is 61.4 BHN, but after adding 8 wt. percent B_4C particles, it is 95.6 BHN. The hardness of B_4C composites using Al2214 alloy-8 wt.% improved by 55.7%. The incidence of hard B_4C particles in the ductile matrix increases the hardness of Al2214 alloy. B_4C particles have a hardness of 3300 BHN, and incorporating such a high-hardness substantial into a soft medium helps to improve the hardness. In addition, because the thermal co-efficient mismatch between the Al2214 alloy and the B_4C particles causes dislocation density, this approach causes higher strain hardening in the composites [27,28]. The composites' hardness is increased through the strain hardening phenomenon.

3.3 Ultimate tensile and yield strength

Figure 9 and Table 3 depict the effect of B_4C addition on the strength of Al2214 alloy. The strength of the Al2214 alloy has been increased by adding 8 weight percent of B_4C particles to the soft Al matrix, as shown in Figure 9. Al2214 alloy has an ultimate tensile strength of 224.8 MPa. In addition, the UTS of Al2214-8 wt.% of B_4C composite is 311.5 MPa. After incorporating 8 wt.% of nano-sized B_4C particles into Al2214 alloy, the UTS improved by 38.5%.

Figure 10 and Table 4 show the effect of B_4C addition on the yield strength of Al2214 alloy. The strength of the Al2214 has been increased by 8 weight percent of B_4C particles in the soft Al matrix, as shown in Figure 10. Al2214 alloy has yield strength of 174.5 MPa. In addition,

Table 2. Hardness of Al2214 alloy and B_4C composites.

Sl No.	Material	Reading I (BHN)	Reading II (BHN)	Reading III (BHN)	Average Hardness (BHN)
1	Al2214 Alloy	59.2	61.2	63.8	61.4
2	Al2214–8 wt.% of B_4C	96.5	95.8	94.7	95.7

Table 3. Ultimate tensile strength of Al2214 alloy and B_4C composites.

Sl No.	Material	Reading I (MPa)	Reading II (MPa)	Reading III (MPa)	Average Ultimate Strength (MPa)
1	Al2214 Alloy	223.6	229.2	221.8	224.8
2	Al2214–8 wt.% of B_4C	311.3	313.6	309.8	311.6

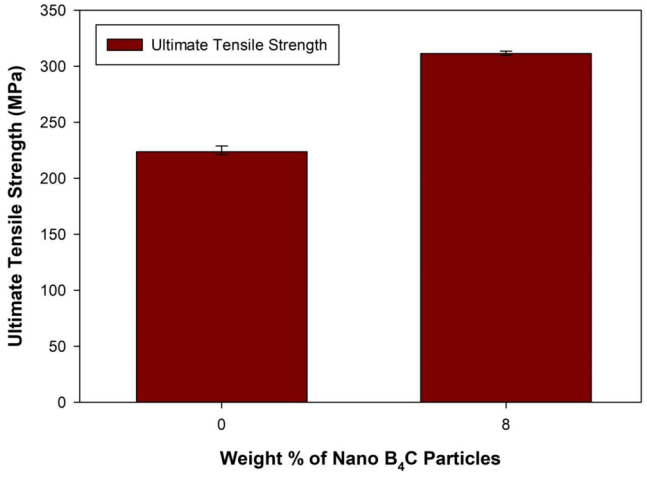

Fig. 9. Ultimate strength of Al2214alloy and B_4C reinforced composites.

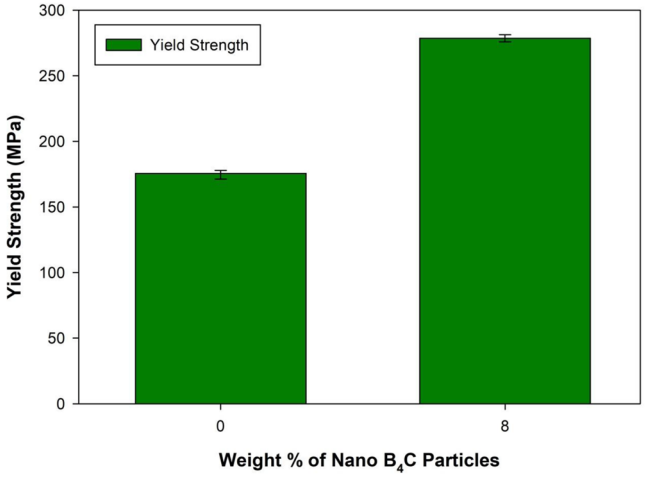

Fig. 10. Yield strength of Al2214 alloy and its composites.

the YS of Al7049-8 wt.% of B_4C composites is 253.7 MPa. After incorporating 8 wt.% of B_4C nano particles into Al2214 alloy, the YS improved by 45.4%.

The ultimate and yield strength of Al2214 alloy were both improved with 8 wt.% of B_4C particles, as shown in plots 9 and 10. The inclusion of the B_4C element in the matrix increases the strength of Al alloy. The hard particle converts the Al matrix brittle, allowing it to withstand higher directed loads. These B_4C bits operate as load-bearing elements in composites, enhancing the composites' strength. Furthermore, according to the Hall-Petch strengthening process, the insertion of tiny particles in the Al matrix reduces the grain size of the composites, which adds to the material's increased strength. The temperature mismatch between the Al2219 and the B_4C particles is large, resulting in density dislocations according to the Orowan principle [29]. Within the Al- B_4C melt, the produced density dislocations cause strain hardening, which leads to the creation of increased strength [30]. Chandrasekhar et al. [31] studied the nano B_4C reinforced Al7475 alloy composites mechanical behavior. Al7475 alloy mechanical properties were improved the incorporation of nano particles.

3.4 Percentage elongation

The ductility of Al2214 alloy and Al2214 alloy with 8 wt.% of B_4C nano composites is shown in Figure 11 and Table 5. According to the graph, ductility reduces by adding B_4C in the matrix. The decrease in ductility is due to the presence of hard B_4C particles in the matrix, as well as significant multidirectional stresses at the Al2214 alloy B_4C contact, which prevents further material elongation. The sound bonding of Al and B_4C particles, as well as the efficient transfer of applied load to a larger number of nano B_4C particles. As a result of all of these effects, the elongation produced in Al2214 alloy − 8 wt.% of B_4C composites is lower than in base amalgam.

3.5 Compression strength

Figure 12 and Table 6 depict the compression strength of Al2214 and Al2214 alloy with 8 wt.% of B_4C particles reinforced composites. The existence of rigid particle phase increased the compression strength of the Al2214 matrix, according to the plot. Because these ceramics are tougher in nature, compressive strength is always used to determine the

Table 4. Yield strength of Al2214 alloy and B_4C composites.

Sl No.	Material	Reading I (MPa)	Reading II (MPa)	Reading III (MPa)	Average Yield Strength (MPa)
1	Al2214 Alloy	175.6	177.1	170.8	174.5
2	Al2214–8 wt.% of B_4C	253.6	255.7	251.9	253.7

Table 5. Elongation of Al2214 alloy and B_4C composites.

Sl No.	Material	Reading I (%)	Reading II (%)	Reading III (%)	Average Elongation (%)
1	Al2214 Alloy	14.9	15.1	14.9	14.96
2	Al2214–8 wt.% of B_4C	11.2	11.1	11.2	11.16

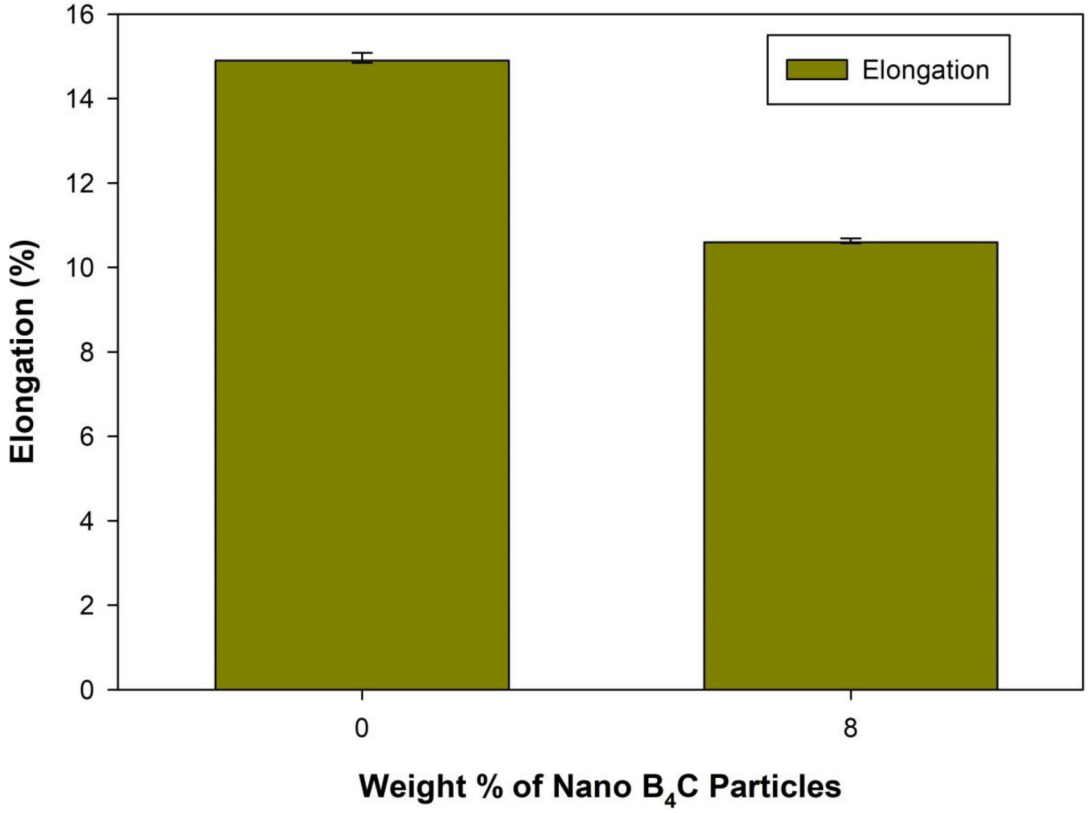

Fig. 11. Ductility of Al2214 alloy and its composites.

strength of the carbide or oxide particles. The large degree of grain refinement gained with the inclusion of B_4C, the incidence of evenly disseminated tougher components, and dislocation created due to the modulus mismatch and thermal expansion co-efficient can all be contributed to the Al-B_4C composites' strength [32]. According to the results of Figure 12, the effect of B_4C content on compressive strength is significant. This demonstrates that B_4C particles have a clear effect on the strength of Al-B_4C composites.

3.6 Tensile fractography

SEM pictures of the breakage surfaces of Al2214 and Al2214 alloy with 8 wt.% of B_4C composites are shown in Figures 13a and 13b. The good bonding between the Al2214 and the B_4C reinforcement can be inferred from all of the tension fractured micrographs. The shattered surface of 500X magnification photos of Al2214 alloy is shown in Figure 13a. The ductile fracture is shown by the cracked surface of the as cast alloy, which has clear visibility of the grains.

Figure 13b shows the fractured surfaces of B_4C reinforced composites, which have brittleness due to the presence of B_4C reinforcement. Furthermore, the brittle fracture is directly connected to the composites' elongation. The ductility of the composites decreases as the weight percent of B_4C particles increases, as discussed in the percentage elongation section.

Table 6. Compression strength of Al2214 alloy and B_4C composites.

Sl No.	Material	Reading I (MPa)	Reading II (MPa)	Reading III (MPa)	Average Compression Strength (MPa)
1	Al2214 Alloy	535.2	543.2	538.9	539.1
2	Al2214–8 wt.% of B_4C	751.4	749.3	756.8	752.5

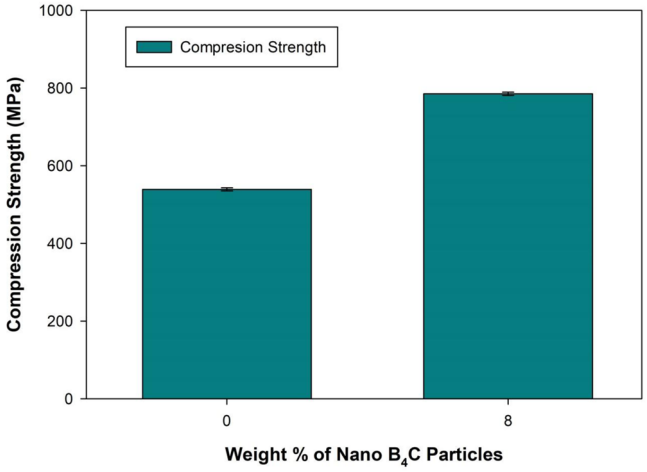

Fig. 12. Compression strength of Al2214 alloy and its composites.

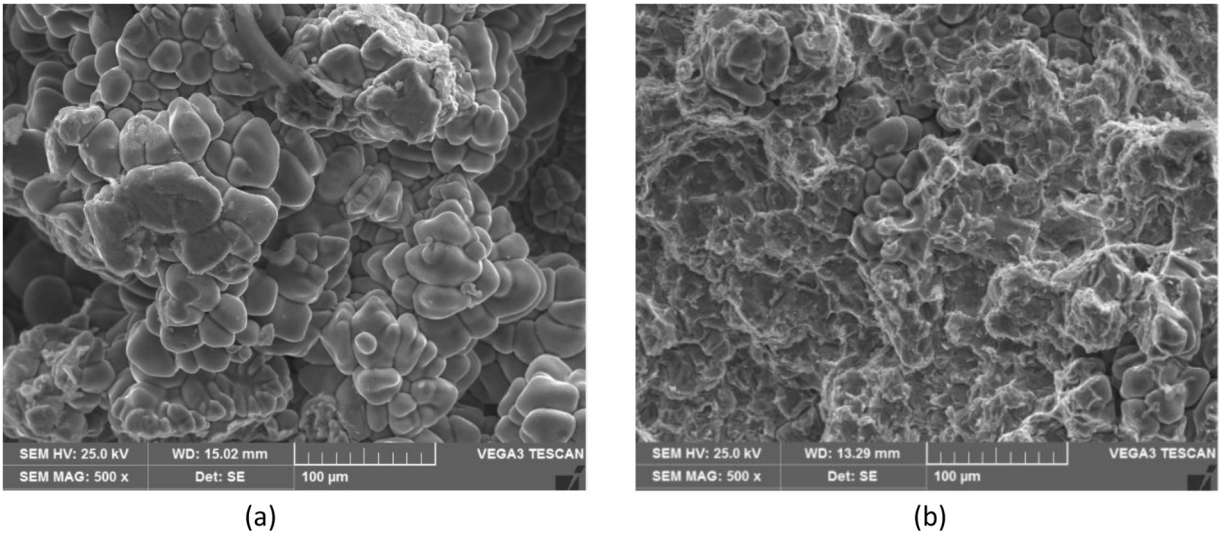

Fig. 13. Fractured surfaces SEM images of (a) Al2214 alloy (b) Al2214-8 wt.% B_4C composites.

4 Conclusions

The Al2214 alloy with 8 wt.% of B_4C metal composites were successfully synthesized using the stir casting method. SEM, EDS and XRD patterns were used to examine the microstructural characteristics of the produced Al2214 alloy and Al2214 alloy with 8 wt.% of B_4C nano composites. SEM micrographs, EDS analysis and XRD patterns were used to show the distribution and existence of B_4C nano particles in the Al2214 alloy metal composites. The results showed that with the addition of 8 wt.% of B_4C nano content in the Al2214 alloy, there was increase in the ultimate, yield, and compression strength with a nominal drop in ductility. In unreinforced material, tensile fractured surfaces showed ductile mode fracture. Furthermore, 8 wt.% of B_4C reinforced composites began to shatter in a brittle manner.

References

1. P.R. jadhav, B.R. Sridhar, M. Nagaral, J.I. Harti, Mechanical behavior and fractography of graphite and boron carbide particulates reinforced A356 alloy hybrid metal matrix composites, Adv. Compos. Hybrid Mater. **3** (2020) 114–119
2. P.H. Nayak, H.K. Srinivas, M. Nagaral, Characterization of tensile fractography of nano ZrO_2 reinforced copper-zinc alloy composites, Frattura ed Integrity Strutturale (Fracture and Structural Integrity) **48** (2019) 370–376
3. M. Nagaral, S. Kalgudi, V. Auradi, S. Kori, Mechanical characterization of ceramic nano B_4C-Al2618 alloy composites synthesized by semi solid processing, Trans. Indian Ceram. Soc. **77** (2018) 1–4
4. N.G. Siddesh Kumar, G.S. Shivashankar, S. Basavarajappa, R. Suresh, Some studies on mechanical and machining characteristics of Al2219/n-B_4C/MoS_2 nano hybrid metal matrix composites, Measurement **107** (2017) 1–11
5. C.S. Ramesh, R. Noor Ahmed, M.A. Mujeebu, M.Z. Abdullah, Development and performance analysis of novel cast copper SiC-Gr hybrid composite, Mater. Des. **30** (2009) 1957–1965
6. V. Bharath, M. Nagaral, V. Auradi, Preparation, characterization and mechanical properties of Al_2O_3 reinforced 6061 Al particulate MMCs, Int. J. Eng. Res. Technol. **1** (2012) 1–6
7. V. Hiremath, S.T. Dundur, R.L. Bharath, G.L. Rajesh, V. Auradi, Studies on mechanical and machinability properties of B_4C reinforced 6061 aluminium MMC produced via melt stirring, Appl. Mech. Mater. **592** (2014) 744–748
8. M. Nagaral, V. Auradi, K.I. Parashivamurthy, S.A. Kori, B.K. Shivananda, Synthesis and characterization of Al6061-SiC-Graphite composites fabricated by liquid metallurgy, Mater. Toady Proc. **5** (2018) 2836–2843
9. M. Nagaral, V. Auradi, V. Bharath, S. Patil, M.S. Tattimani, Effect of micro graphite particles on the microstructure and mechanical behavior of aluminium 6061 (Al-Mg-Si) alloy composites developed by novel two step casting technique, J. Metals Mater. Minerals **31** (2021) 38–45
10. V. Bharath, V. Auradi, M. Nagaral, S.B. Boppana, S. Ramesh, K. Palanikumar, Microstructural and wear behavior of Al2014-alumina composites with varying alumina content, Trans. Indian Inst. Metals **75** (2022) 133–147
11. H.S. Kumar, U.N. Kempaiah, M. Nagaral, V. Auradi, Impact, tensile and fatigue failure analysis of boron carbide particles reinforced Al-Mg-Si (Al6061) alloy composites, J. Failure Anal. Prevent. **21** (2021) 2177–2189
12. R.A. Chennakesava, Tensile fracture behaviors of 7072/SiCp metal matrix composites fabricated by gravity die casting process, Mater. Technol. **26** (2011) 257
13. R.M. Wang, M.K. Surappa, C.H. Tao, C.Z. Li, M.G. Yan, Microstructure and interface structure studies of SiC reinforced Al6061 metal matrix composites, Mater. Sci. Eng. A **254** (1998) 219–226
14. S.A. Sajjadi, M. Torabi Parizi, H.R. Ezatpour, A. Sedghi, Fabrication of A356 composite reinforced with micro and nano Al_2O_3 particles by a developed compo-casting method and study of its properties, J. Alloys Compd. **511** (2014) 226–231
15. G.L. Chandrasekhar, Y. Vijayakumar, M. Nagaral, C. Anilkumar, Microstructural evaluation and mechanical behaviour of nano B_4C reinforced Al7475 alloy metal composites, Int. J. Vehicle Struct. Syst. **13** (2021) 673–677
16. M. Nagaral, V. Auradi, S.A. Kori, H.N. Reddappa, Jayachandran, V. Shivaprasad, Studies on 3 and 9 wt.% of B_4C particulates reinforced Al7025 alloy composites, AIP Conf. Proc. **1859** (2017) 020019
17. D. Patidar, R.S. Rana, Effect of B_4C reinforcement on the various properties of aluminium matrix composites: a survey paper, Mater. Today Proc. **4** (2017) 2981–2988
18. G.B. Veereshkumar, Assessment of mechanical and tribological characteristics of silicon nitride reinforced aluminium metal matrix composites, Compos. Part B: Eng. **175** (2019) 107138
19. H.S. Vasanth Kumar, U.N. Kempaiah, M. Nagaral, K. Revanna, Investigations on mechanical behaviour of micro B_4C particles reinforced Al6061 alloy metal composites, Indian J. Sci. Technol. **14** (2021) 1855–1863
20. V.A. Anjan Babu, R. Saravanan, M. Raviprakash, M. Nagaral, Microstructure, tensile and flexural strength of boron carbide particles reinforced Al2030 alloy composites, Indian J. Sci. Technol. **14** (2021) 2342–2350
21. M. Nagaral, V. Auradi, V. Bharath, Mechanical characterization and fractography of 100 micron sized silicon carbide particles reinforced Al6061 alloy composites, Metall. Mater. Eng. (2021). https://doi.org/10.30544/639
22. J.I. Harti, B.R. Sridhar, H.R. Vitala, P.R. Jadhav, Wear behavior of Al2219-TiC particulate metal matrix composites, Am. J. Mater. Sci. **5** (2015) 34–37
23. S. Matti, B.P. Shivakumar, S. Shashidhar, M. Nagaral, Dry sliding wear behavior of mica, fly ash and red mud particles reinforced Al7075 alloy hybrid metal matrix composites, Indian J. Sci. Technol. **14** (2021) 310–318
24. T. Rajmohan, K. Palanikumar, S. Ranganathan, Evaluation of mechanical and wear properties of hybrid aluminium matrix composites, Trans. Nonferrous Metals Soc. China **23** (2013) 2509–2517
25. M. Nagaral, V. Auradi, S.A. Kori, V. Hiremath, Investigations on mechanical and wear behavior of nano Al2O3 particulates reinforced AA7475 alloy composites, J. Mech. Eng. Sci. **13** (2019) 4623–4635
26. K. Kalaiselvan, N. Murugan, S. Parameshwaran, Production and characterization of AA6061-B_4C stir cast composite, Mater. Des. **32** (2011) 4004–4009
27. P.R. Jadhav, M. Nagaral, S. Rachoti, J. Harti, Impact of boron carbide and graphite dual particulates addition on wear behavior of A356 alloy metal matrix composites, J. Metals Mater. Minerals **30** (2020) 106–112
28. T.H. Raju, R.S. Kumar, S. Udayashankar, A. Gajakos, Influence of dual reinforcement on mechanical characteristics of hot rolled AA7075/Si3N4/graphite MMCs, J. Inst. Eng. Ser. D **102** (2021)
29. T. Hemanth Raju, B.B. Chandan, S. Belagavi Vinaya, T.J. Udayashankar, A.K. Gajakosh, Influence of zircon particles on the characterization of Al7050-Zircon composites, Mater. Today Proc. **47** (2021)
30. U.B. Krishna, B. Vasudeva, V. Auradi, Ma. Nagaral, Mechanical characterization and tensile fractography of Al7075-WCP-CoP composite, Frattura e Integrita Strutturale **60** (2022)

31. G.L. Chandrasekhar, Y. Vijayakumar, M. Nagaral, C. Anilkumar, Microstructural evolution and mechanical behavior of 8 wt.% of nano B_4C reinforced Al7475 alloy metal composites, Int. J. Vehicle Struct. Syst. **13** (2021) 1–6

32. Z. Ali, V. Muthuraman, P. Rathnakumar, P. Gurusamy, M. Nagaral, Studies on mechanical properties of 3 wt.% of 40 and 90 μm size B_4C particulates reinforced A356 alloy composites, Mater. Today: Proc. **52** (2022) 494–499

Cite this article as: Kumar Gopalan, Saravanan Rajabathar, Madeva Nagaral, Hemanth Raju Thippeswamy, Evaluation of mechanical behaviour and tensile failure analysis of 8 wt.% of nano B_4C particles reinforced Al2214 alloy nano composites, Manufacturing Rev. **9**, 31 (2022)